The final publication is available at

http://doi.org/10.1111/j.1365-313X.2012.05046.x

Additional Information

Functional analyses of AGAMOUS family members in *Nicotiana benthamiana* clarify the evolution of early and late roles of C-function genes in eudicots

Chloe Fourquin and Cristina Ferrándiz*

Instituto de Biología Molecular y Celular de Plantas (IBMCP), UPV-CSIC.

Av. de los Naranjos s/n 46022 Valencia, Spain

* For correspondence :

Cristina Ferrándiz

Instituto de Biología Molecular y Celular de Plantas, UPV-CSIC

Campus de la Universidad Politécnica de Valencia, 46022 Valencia, Spain

Tel. +34 963877892; Fax +34 963877859; e-mail: cferrandiz@ibmcp.upv.es

Additional e-mail addresses: Chloe Fourquin: chloef@ibmcp.upv.es

SUMMARY

The C-function, according to the ABC model of floral organ identity, is required for stamen and carpel development and to provide floral meristem determinacy. Members of the AG lineage of the large MADS-box gene family specify the C-function in a broadly conserved manner in Angiosperms. In core eudicots, two sublineages coexist, euAG and PLE, extensively characterized in *Antirrhinum majus* and *Arabidopsis thaliana*, where strong subfunctionalization has led to highly divergent contributions of the respective paralogs to the C-function. Different scenarios have been proposed to reconstruct the evolutionary history of the euAG and PLE lineages in eudicots, but detailed functional analyses of the role of these genes in additional representative species to validate evolutionary hypotheses are scarce. Here, we report the functional characterization of the euAG- and PLE-like genes in *Nicotiana benthamiana* through expression analyses and phenotypic characterization of the defects caused by their specific downregulation. We show that both paralogs redundantly contribute to the C-function in this species, providing insights on the likely evolution of these gene lineages following the divergence of the major groups within the eudicots (rosids and asterids). Moreover, we have shown a conserved role of the PLE-like genes in controlling fruit dehiscence, which strongly supports the ancestral role of PLE-like genes in late fruit development and suggests a common evolutionary origin of late developmental processes in dry (dehiscence) and fleshy (ripening) fruits.

INTRODUCTION

A major factor for the evolutionary success of the Angiosperms, consisting of more of 300,000 extant species, is the carpel. Carpels protect the ovules, provide support for pollenization, including incompatibility mechanisms, and, after fertilization, develop into fruits, which in turn protect the developing seeds and ensure seed dispersal. Understanding the evolution and functional diversifications of carpels and fruits is therefore a fundamental question in Evo-Devo studies.

Carpel identity in Angiosperms is specified by C-function genes, as defined by the ABC model of floral organ identity (Coen and Meyerowitz 1991). C-function, in addition to providing carpel identity in the central whorl of the flower, specifies stamen identity in combination with B-function genes in whorl 3 and also control floral meristem determinacy. Members of the AG lineage of the large MADS-box gene family specify the C-function in a broadly conserved manner, as revealed by many functional studies including the characterization of mutant or knockdown lines in monocots, and in basal and core eudicots (Bowman *et al.* 1989, Bradley *et al.* 1993, Davies *et al.* 1999, Dreni *et al.* 2011, Mena *et al.* 1996, Pan *et al.* 2010, Pnueli *et al.* 1994, Yellina *et al.* 2010).

In core eudicots, the C-class genes were identified in *Arabidopsis thaliana* and in *Antirrhinum majus*, where they have been thoroughly characterized. In both species, the C-function is mainly carried out by a single AG-like gene, *AGAMOUS* (which we will refer to as *AtAG* for clarity) in *Arabidopsis* and *PLENA* (*AmPLE* hereafter) in *Antirrhinum*. *AtAG* and *AmPLE* encode closely related genes whose expression start early in the floral sexual organ primordia and remain specific to the carpel and stamens throughout their development. In loss-of-function mutants of these genes the sexual organs are totally absent in the flower and are replaced by several whorls of sepals and petals (Bowman *et al.* 1989; Bradley *et al.* 1993).

AtAG and *AmPLE* belong to the MADS box AG-subfamily, although they are not orthologous genes. A major duplication event took place early in the history of the core

eudicots that led to the origin of two gene lineages within the AG subfamily: euAG and PLE (Kramer *et al.* 2004). In *Arabidopsis*, a member of the rosids, the C-function gene *AtAG* corresponds to the euAG lineage while in *Antirrhinum*, a member of the asterids, the C-function gene *AmPLE* corresponds to the PLE lineage. The PLE lineage genes in *Arabidopsis* are the two *SHATTERPROOF* genes (*AtSHP* hereafter), products of a very recent duplication within the Brassicaceae. In contrast with their paralog *AtAG*, *AtSHP* genes do not contribute significantly to the C-function, since the only phenotype observed in the double mutant *shp1shp2* is a late defect in fruit dehiscence (Liljegren *et al.* 2000). Likewise, in *Antirrhinum*, the *euAG* lineage is represented by *FARINELLI* (*AmFAR* hereafter), which appears to provide only a minor contribution to C-function in pollen development (Davies *et al.* 1999).

These studies suggested an evolutionary scenario where a functional switch between the euAG and PLE lineages to specify C-function and the subfunctionalization of *SHP* genes to control fruit dehiscence occurred after the divergence of the asterids and the rosids (Causier *et al.* 2005). This functional switch has been subsequently attributed to changes both in gene regulation and protein activity. The floral regulator gene *LEAFY* (*LFY*) is a key activator of *AtAG* and promotes its very early expression in the center of the flower meristem (Busch *et al.* 1999, Parcy *et al.* 1998). A reduced response to LFY activation in *AtSHP* and *AmFAR* has then been suggested as an explanation for their minor participation in the C-function (Moyroud *et al.* 2011). In addition, a single amino acid difference between AmPLE and AmFAR (Q173 insertion in AmFAR) has been identified as a key element to explain the functional differences of the two proteins (Airoldi *et al.* 2010). All together, these results indicate that primary C-function has been retained by a different member of the gene pair in *Arabidopsis* and *Antirrhinum*, and maybe more generally in rosids and asterids, and enlighten the plasticity of functional evolution following gene duplication (Causier *et al.* 2005).

However, several functional analyses conducted in the asterid family of Solanaceae provide conflicting results that undermine this hypothesis on C-function evolution, at least regarding the timing of evolutionary events. In petunia, tomato and tobacco, euAG orthologs appear to be significantly involved in stamen and carpel specification, as well as in the control of meristem determinacy (Kapoor *et al.* 2002, Kempin *et al.* 1993, Pan *et al.* 2010, Pnueli *et al.*1994). Thus, the reduced contribution of the euAG ortholog to the C-function could be restricted to *AmFAR* in the *Antirrhinum* lineage. However, a complete loss-of-C-function phenotype has not been observed in the reported experiments where euAG orthologs have been downregulated in Solanaceae, strongly suggesting that other genes participate in the C-function in these species, for which PLE genes are obvious candidates. Little information is available on the function of the PLE lineage genes outside *Arabidopsis* and *Antirrhinum*. In tomato (asterid), downregulation of the PLE-like gene *TAGL1* has been shown to affect fruit ripening, but not to cause defects in floral organ specification (Giménez *et al.* 2010, Pan *et al.* 2010, Vrebalov *et al.* 2009). Thus, the role of *TAGL1* appears to be restricted to late fruit development, similar to what has been described for the PLE-like *SHP* genes in Arabidopsis. Likewise, expression studies in different peach varieties (rosids) suggest a role of *PLE* orthologs in fruit ripening and lignification of pericarp cells (Tani *et al.* 2007). These studies may indicate that the *PLE* genes could have a reduced early role in floral organ specification and a more prominent role late in fruit development, not specific to the *Arabidopsis* lineage but more generally conserved in other eudicots. However, the profound structural differences between fleshy berries (tomato, peach) and dry dehiscent fruits (*Arabidopsis*), together with the lack of additional examples of mutants in PLE-lineage genes, hamper the validity of these speculations.

Therefore, the reported studies on AG-lineage genes in core eudicots leave open relevant questions. First, it remains to be studied whether PLE-like genes significantly contribute to C-function in species other than *Antirrhinum*. In this sense, it is currently

not clear whether expression studies coupled to regulatory sequence analyses have a good predictive value in assessing the relative contribution of AG-like genes to C-function and can be used to formulate evolutionary hypotheses. Finally, a more general question is whether the late role of PLE-like genes controlling dehiscence predates the divergence of rosids and asterids. This putative ancestral role of PLE lineages genes in late fruit development may therefore indicate a common developmental origin of dehiscence and fruit ripening in dry and fleshy fruits respectively.

Here, we report a detailed functional analysis of the euAG- and PLE-like genes in a Solanaceae species, *Nicotiana benthamiana*, aiming to unravel their respective contributions to C-function and therefore to better understand the evolution of these gene lineages following the divergence of the rosids and asterids. In addition, as *Nicotiana* forms dry and dehiscent fruits, it has allowed us to gather deeper insights into the function of the PLE-like genes in fruit development and possibly fruit evolution.

RESULTS

To functionally characterize the *euAG* and *PLE* genes in *Nicotiana benthamiana*, we cloned the corresponding full-length likely orthologs by RT-PCR from cDNA of young flowers using available sequence information of AG-like genes from the close relative *Nicotiana tabaccum* from public databases (*NAG1* and *NtPLE36*, see methods). NbAG shows 96% aa identity with NAG1, and is more similar to *Arabidopsis* AtAG (67% identity) or *Antirrhinum* AmFAR (79% of identity) than to AtSHP or AmPLE. NbSHP shows 67% and 64% identity to AtSHP1 and AtSHP2, respectively, and 76% to AmPLE. The phylogenetic analysis shown in Figure 1a clearly groups NbAG in the euAG clade, and NbSHP in the PLE clade.

The large second intron of euAG/PLE genes has been shown to be important for their regulation and to contain several conserved motifs, including a LFY binding site reported as critical to establish early expression in flower development of C-function

genes, and two other motifs, an aAGAAT box and a 70 bp element characterized by a CCAATCA repeat (Causier *et al.* 2009). Because the presence of these conserved motifs has been suggested to have some predictive value on the relative contribution of AG-like genes to C-function in different species (Moyroud *et al.* 2011), we analyzed the sequences of the second intron of *NbAG* (3897 kb) and *NbSHP* (2742 bp). We found *NbAG* and *NbSHP* second introns to have the conserved aAGAAT box and the 70 bp element. A consensus binding site for LFY (CCANTGG, as defined in Hong et al., 2003 and Causier et al., 2005) was found in *NbAG* intron but not in *NbSHP*, suggesting that *NbSHP* might have lost the early onset of expression and therefore might have a reduced role in C-function (Figure S1). However, we also made use of a bioinformatic tool based on a biophysical model that quantitatively predicts LFY affinity for specific genomic regions (termed "Predicted occupancy" or POcc), outperforming the classical search of consensus binding sites (Moyroud *et al.* 2011). Interestingly, we found a high level of LFY POcc in both *NbAG* and *NbSHP* second introns, being significantly higher for the later, similar to what has been reported for the pair *AmFAR*/*AmPLE* from *Antirrhinum* and opposite to *AtAG*/*AtSHP* in *Arabidopsis* (Figure 1b and S1).

In addition to the role of *cis*-elements in the evolution of C-function genes, a single glutamine insertion in the sequence of AmFAR protein has been correlated to its possible subfunctionalization in mainly specifying male organ identity. Examination of both NbAG and NbSHP amino acid sequences showed that both deduced proteins lacked this glutamine residue, thus suggesting that functional differences between NbAG and NbSHP proteins produced by this aminoacid change should not be expected.

In summary, sequence analyses of *NbAG* and *NbSHP* suggested that both factors could share C-function specification, although *NbSHP* may have a more prominent early role based on predicted LFY occupancy of the second intron.

NbAG and *NbSHP* are expressed during floral development like typical C-function genes

To elucidate the detailed expression patterns of *NbAG1* and *NbSHP*, we performed *in situ* hybridization on young buds of *Nicotiana benthamiana*. We used as probes the last 500 bp of each coding sequence, a region presenting low sequence similarity between the two genes (64% versus 81% in the MADS-box coding region). Both *NbAG* and *NbSHP* transcripts began to accumulate at stage 2 of flower development as defined by Mandel *et al.* (1992), when the sepal primordia arise, in the central domain of the flower, which later will give rise to stamen and carpel primordia (Figure 2a and b). At this stage, both transcripts showed similar expression domains, although *NbAG* expression appeared to accumulate more externally in the floral meristem than *NbSHP*. At stage 4, when petal primordia were visible, *NbAG* and *NbSHP* were detected in the cells that would develop into stamens and carpels (Figure 2c and d). At stage 6, *NbAG* and *NbSHP* transcripts were uniformly present in the developing stamens and in the apical central zone of the pistil (Figure 2e and f). In the mature flower, the expression of both genes was weak in stamens but strong in the placenta (Figure 2g and h). In later stages, expression of both transcripts was also observed in the developing ovules (Figure 2i and j).

From these experiments, we can conclude that the expression of these two genes remained specific to the sexual organs from early stages and throughout flower development. *NbAG* and *NbSHP* showed nearly identical temporal and spatial expression patterns, similar to those described for Arabidopsis *AtAG* or Antirrhinum *AmPLE* genes.

Silencing of *NbAG* and *NbSHP* in *N. benthamiana* using VIGS technology differentially affect flower and fruit development

Expression analyses suggested that both *NbAG* and *NbSHP* genes could have similar early and late roles in floral development in *N. benthamiana*. To investigate the specific contribution of each gene to these roles, we used Virus Induced Gene Silencing (VIGS) to reduce *NbAG* and *NbSHP* transcript levels in *N. benthamiana*. This method transiently downregulates the expression of a specific gene via modified plant viruses, in our case the Tobacco Rattle Virus (TRV), and it has been shown to efficiently direct the degradation of endogenous mRNAs in *Nicotiana* as well as other species (Constantin *et al.* 2004, Hileman *et al.* 2005, Ratcliff *et al.* 2001, Wege *et al.* 2007). In order to specifically silence *NbAG* and *NbSHP* genes, we generated TRV constructs carrying the same coding sequence fragments used for the *in situ* analyses, which showed low sequence similarity and did not present contiguous stretches of more than 20 identical nucleotides.

NbAG-VIGS

Twelve plants were inoculated by the TRV2-NbAG construct. To evaluate the efficiency and specificity of the VIGS treatment, the level of *NbAG* and *NbSHP* transcripts were measured by quantitative RT-PCR on flowers from five different treated plants. We observed that in all cases, the expression of *NbAG* was significantly reduced compared to the WT, whereas the expression of *NbSHP* was practically unaffected (Figure S2), proving that the TRV2-NbAG construct was gene specific.

In the wild type flower of *N. benthamiana*, the first whorl is composed by five sepals fused for most of their length; in the second whorl, five petals develop fused in a tubular corolla; the third whorl is composed of five stamens whose long filaments are adnately fused to the second whorl; and the fourth whorl is occupied by a two-carpellate gynoecium. The mature pistil is composed of a short ovary divided into two locules with central placentation, and a very long style, which ends by a round and flat stigma (Figure 3 and 4).

NbAG-VIGS plants showed homeotic transformations specifically restricted to the sexual organs of the flower. This phenotype was observed in approximately 92% of the flowers of all the treated plants. In the third whorl, stamens were replaced by petals (Figure 3b and f). The petals developing in the third whorl were free instead of fused into a tubular structure and in 74% of the flowers there were more than five petals (between 6 and 10) (Figure 4c). In the center of NbAG-VIGS flowers, a short tubular green organ developed, which appeared to have mixed sepal-carpel identity (Figure 3f and k). A closer inspection by SEM confirmed the sepal identity of these structures. Instead of the small and rectangular cells typical of the ovary epidermis (Figure 5e), we found puzzle shaped cells, and numerous trichomes and stomata, which are typical of the sepal abaxial surface (Figure 5c). However, the organs in the fourth whorl of NbAG-VIGS flowers also retained some carpelloid features like stigmatic tissue (Figure 3m and 4h).

In addition to homeotic transformation of stamens and carpels, the NbAG-VIGS treatment caused the indeterminacy of the floral meristem. NbAG-VIGS flowers developed additional whorls of petals and sepals inside the sepalloid gynoecium (Figure 3l). These supernumerary organs were evident in the histological sections of the flower (Figure 4c, h and i). Moreover, the prolonged activity of the floral meristem in the NbAG-VIGS plants occasionally produced an ectopic floral meristem in the center of the flower (Figure 4i).

Our results indicated that *NbAG* had a major role in providing C-function, being required to both specify stamen and carpel identity and to control floral determinacy. However, the presence of carpel tissue in the fourth whorl of all the NbAG-VIGS flowers analyzed also suggested that additional factors, most likely *NbSHP*, could participate in carpel identity specification, or, alternatively, that the residual NbAG activity in the VIGS-treated plants could be sufficient to partly direct carpel development.

NbSHP-VIGS

To functionally characterize *NbSHP* and to specifically evaluate its possible contribution to C-function and to fruit development, we performed an equivalent experiment with a specific TRV-NbSHP construct. The quantification of *NbAG* and *NbSHP* transcripts in treated plants revealed that the expression of *NbSHP* was strongly reduced in the NbSHP-VIGS flowers whereas the expression of *NbAG* was not significantly altered or even increased (Figure S2).

NbSHP-VIGS plants showed phenotypic alterations restricted to flower development. Stamen development was mostly unaffected, although occasionally mild transformations of anthers into petaloid tissue were observed (Figure S4). In contrast, gynoecium development was severely affected in 94% of NbSHP-VIGS flowers. Incomplete carpel fusion led to a complete split of style and stigma. Moreover, the style was much shorter than in the wild type plants (Figure 3c, g, n and 4f). Close inspection of the epidermal cells of the NbSHP-VIGS modified ovary revealed that cell morphology was intermediate between typical ovary and sepal cells, with development of stomata and trichomes, characteristics of sepal tissue (Figure 5e). Stomata and trichomes were also observed on the style epidermis of the NbSHP-VIGS gynoecium (Figure 5f). These observations indicate that a partial homeotic conversion occurred in the fourth whorl of the NbSHP-VIGS flowers.

In addition, most of the NbSHP-VIGS flowers displayed mild to strong defects in floral meristem determinacy. In 43% of the flowers, the gynoecium was formed by more than two carpels and developed internal whorls of carpeloid organs (Figure 3n, 4b and j). Supernumerary organs were also found in the third whorl of 36% of the flowers, where up to 10 stamens developed instead of the typical 5 formed in wild type flowers (Figure 4b).

Although the vast majority of the NbSHP-VIGS gynoecia were severely affected and therefore sterile, fruits were able to develop on a small proportion of NbSHP-VIGS flowers only several weeks after inoculation and allowed us to evaluate the possible role of NbSHP in fruit development. These fruits were anatomically almost identical to wild-type fruits and did not show any sign of homeotic transformations, as revealed by close inspection of ovary cell morphology and of ovary wall organization (Figure S5). The wild-type fruit of *N. benthamiana* is a dry capsule, which opens at maturity to allow seed dispersal along four dehiscence zones at the top of the fruit that correspond to the two fused carpel margins and to the central carpel midveins (Figure 6a). In contrast, all the NbSHP-VIGS fruits that were formed remained indehiscent even weeks after maturity, a phenotype similar to that caused by loss of function of *AtSHP* genes in Arabidopsis (Figure 6b). It is known that lignification of dehiscence zones plays a crucial role in fruit shattering and that dehiscence zone lignification is greatly reduced in Arabidopsis *shp1shp2* mutants (Liljegren *et al.* 2000). For this reason, we studied the lignification pattern in NbSHP-VIGS mature fruits compared to wild type. In the wild type fruit, four strongly lignified narrow stripes were observed at the top of the fruit, which corresponded to the dehiscence zones (Figure 6c). By contrast, no lignification was detected along the fused carpel margins or the midveins of the carpels in the indehiscent NbSHP-VIGS fruits (Figure 6d).

NbAG1-NbSHP-VIGS

In addition to its role in fruit dehiscence, the described phenotypes of NbSHP-VIGS plants indicated that this gene seemed to play a major role in the control of meristem determinacy, while also participating in the specification of carpel identity and, to a lesser degree, of stamen identity. In this sense, *NbSHP* appeared to be responsible for the presumptive residual C-function in NbAG-VIGS flowers. Thus, in order to see if the downregulation of *NbSHP* modified the NbAG-VIGS phenotype, we silenced both

genes simultaneously inoculating 12 plants with the TRV2-NbAG-NbSHP vector. Quantitative PCR in the flowers of five treated plants confirmed that both genes were strongly downregulated (Figure S2).

95% of the NbAG-NbSHP-VIGS flowers completely lacked stamens and carpels, and showed a greatly enhanced floral indeterminacy compared to the specific downregulation of the individual genes. Sepals and petals developed normally, although occasionally some supernumerary organs were observed (Figure S4). In the third whorl, stamens were converted into petals (Figure 3d). In 90% of the flowers, a new tubular corolla of petals developed in the fourth whorl, which enclosed numerous petals reiterating the pattern in second and third whorls (Figure 3h and 4d). However, around 5% of the flowers showed a different phenotype: instead of the fourth whorl a new flower developed composed of sepals and petals (Figure 3i), similar to what has been described for *Arabidopsis ag* mutants (Bowman et al., 1989). In very few flowers, an ectopic flower emerging from the axil of a third whorl organ was also observed (Figure 3o), suggesting that *NbAG* and *NbSHP* could also have a minor role in floral meristem specification.

DISCUSSION

In this work, we present a detailed characterization of the role of AG-like genes from euAG and PLE lineages in flower and fruit development in the Solanaceae species *Nicotiana benthamiana*. Our studies provide additional data to address several open questions regarding the evolution of AG-like genes in eudicots. First, we have been able to assess the specific contribution of a member of the PLE-lineage in asterids to the C-function. Second, our results help to understand the temporal and quantitative requirements of AG-like factors to the different aspects of C-function. Finally, we have

shown the conserved role of PLE-like genes in the regulation of fruit dehiscence in distantly related species.

The C-function in *Nicotiana benthamiana*

Previous works performed in other Solanaceae species like petunia or tomato suggested that, in contrast to the situation in *Arabidopsis* or *Antirrhinum*, both paralogs from the PLE and euAG lineages could be significantly required to contribute to the C-function (Kapoor *et al.* 2002, Pan *et al.* 2010, Vrebalov *et al.* 2009). However, functional data, especially for PLE-like genes, were only partial and were therefore insufficient to fully confirm this hypothesis. In this work, we demonstrate that both *NbAG* (euAG lineage) and *NbSHP* (PLE lineage) genes jointly carry out the C-function in the Solanaceae species *Nicotiana benthamiana*.

Simultaneous dowregulation of both *NbAG* and *NbSHP* genes caused typical C-loss-of-function phenotypes, with complete homeotic transformation of stamens into petals, lack of carpels, and loss of floral determinacy, with formation of numerous concentric whorls of petals or new flowers arising from the center of the floral meristem. The specific contribution of *NbAG* and *NbSHP* to these phenotypes was also assessed: *NbAG* but not *NbSHP* appeared to contribute significantly to stamen identity; both *NbAG* and *NbSHP* were required to confer carpel identity, although specific downregulation of *NbAG* had a stronger effect; and both *NbAG* and *NbSHP* controlled similarly floral meristem determination.

In *Arabidopsis* and *Antirrhinum*, where functional studies are extensive and allelic series are available, it has been shown that the different components of the C-function (stamen identity, carpel identity and determinacy) can be genetically separated (Causier *et al.* 2009, Davies *et al.* 1999, Mizukami and Ma 1992). The phenotypes of weak mutant alleles of *AtAG* or *AmPLE* genes support a threshold model in which stamen identity, carpel identity and floral meristem determinacy would each require

different increasing levels of C-function activity. In addition, temporal requirements can be deduced from the phenotypes of heterochronic alleles of *AmPLE*, which indicate that an early onset of expression is needed to specify stamen identity, while correct carpel formation and meristem termination still can be achieved if C-function activation is only attained at later stages of floral development (Causier *et al.* 2009). In this work we show that *NbAG* and *NbSHP* exhibit highly similar temporal and spatial patterns of expression, in partial agreement with the presence of previously described regulatory elements in the second intron of both genes that predict early onset of expression for both, although quantitatively higher for *NbSHP* (Causier *et al.* 2009, Moyroud *et al.* 2011). Since *NbSHP* downregulation shows little or no effect on stamen formation and only causes mild loss of carpel identity, it can be proposed that the different quantitative contribution of both genes to the C-function may rely on differences in protein activity, compatible with the threshold model. In fact, this hypothesis is indirectly supported by the phenotypes of Petunia plants overexpressing *pMADS3* (the *Petunia hybrida* euAG-like gene, 91% identical in deduced aa sequence to NbAG) or *FBP6* (*Petunia hybrida* PLE-like gene, 90% identical to NbSHP): while pMADS3 overexpression induced homeotic transformations of sepals and petals, FBP6 overexpression did not (Kater et al, 1998), therefore indicating that the two proteins had different biochemical potential. Our results indicate that in *N. benthamiana NbAG* and *NbSHP* would be redundantly required for C-function, but *NbAG* would provide higher activity, probably reflecting differences in protein function. Thus, *NbAG* alone would provide enough C-activity to specify stamen identity, while *NbSHP* would not in the absence of *NbAG*; the higher requirements of C-function for carpel specification would need both *NbAG* and *NbSHP*, but the absence of the less active NbSHP factor would only cause mild defects; and finally, only simultaneous expression of both *NbAG* and *NbSHP* would provide sufficient C-activity to promote floral meristem termination.

These conclusions, not anticipated from expression or *in silico* analyses, highlight the importance of functional data to address evolutionary questions and to validate the predictions based on bioinformatic analyses of regulatory sequences to formulate evolutionary hypotheses.

The evolution of C-function

The redundancy of euAG and PLE genes in Nicotiana adds valuable information to clarify the evolution of C-function in eudicots. Expression patterns, protein activities and relative contributions to the C-function for the euAG/PLE paralogs in *Arabidopsis*, *Antirrhinum* and *Nicotiana* are different in each species,

 Together with similar evidence in monocots or basal dicots where AG-like genes have independently diversified but also redundantly provide the C-funcion (Dreni *et al.* 2011, Yellina *et al.* 2010, Zahn *et al.* 2006), it strongly supports an scenario where the subfunctionalization of AG-like genes to carry out the different aspects of C-function would have occurred multiple times in evolution involving both changes in expression patterns and protein activity.

Interestingly, we have observed that the reduction of *NbSHP* mRNA levels in VIGS-treated plants frequently produces a concommitant increase in *NbAG* mRNA levels. Similar effects were previously reported for other species (Davies et al. 1999, Giménez et al. 2010, Kapoor et al. 2002, Vrebalov et al. 2009) suggesting that the ancestral C-function would be autoregulated and that this regulation would have been maintained following duplication. Thus, the autoregulation of C-function genes could provide a compensation mechanism that would facilitate the independent subfunctionalization of duplicated C-function genes.

An ancestral role of PLE genes in late carpel development

In addition to its phenotype in sexual organ identity and in floral meristem maintenance, NbSHP-VIGS flowers show defects in late pistil development, with carpels unfused in the style and stigma regions. In *Arabidopsis*, a recent study has uncovered a similar late role of *AtSHP* genes in the promotion of the apical regions of the pistil, although it is only observed in certain mutant backgrounds (Colombo *et al.* 2010). Thus, as PLE-like genes appear to share a common role in style and stigma development in both *Arabidopsis* and *Nicotiana*, it is possible to speculate that this function is ancestral and was already present in the PLE lineage before the separation of the asterids and the rosids. However, it is difficult to assess if this role is specific to the PLE lineage, or whether euAG-like genes could also participate in this function. Carpel development in NbAG-VIGS is strongly affected and only patches of stigmatic tissue develop. Likewise, *ag* mutants do not form any carpels in Arabidopsis, and therefore, late roles of *AtAG* in pistil development are bound to go unnoticed. The fact that *AtAG* and *AtSHP* genes are expressed in the apical regions of the developing pistil, together with the absence of evident style defects in *shp1shp2* mutants, may also support an alternative scenario where the three genes could redundantly regulate this function.

An ancestral role of PLE lineage genes in fruit development

In addition to the different floral phenotypes discussed above, we show that the downregulation of the *NbSHP* gene leads to the development of indehiscent fruits with strongly reduced lignification at the presumptive dehiscence zone. Remarkably, these fruits phenocopy the *shp1shp2* double mutants in *Arabidopsis* (Liljegren *et al.* 2000). The fruit shattering process is well documented in *Arabidopsis* (for review see Ferrándiz 2002, Ferrandiz *et al.* 2010). The *AtSHP* genes are expressed in the valve margins and later in the fruit dehiscence zones, where they are required for

differentiation of the dehiscence zone in the *Arabidopsis* silique and the lignification of the adjacent cells. *AtSHP* expression is restricted to the valve margins by the negative regulation exerted by *FRUITFULL* (*AtFUL*), another member of the MADS box family from the AP1/FUL clade expressed in the valves. In *Arabidopsis*, *AtFUL* overexpression phenocopies the *shp1shp2* mutant, resulting in indehiscent fruits with reduced lignin (Ferrándiz *et al.* 2000). The *FUL* ortholog of *Nicotiana tabacum*, *NtFUL*, has been previously studied. When *NtFUL* is overexpressed in the related species *Nicotiana sylvestris*, indehiscent fruits are also formed (Smykal *et al.* 2007). Thus, both in *Arabidopsis* and in *Nicotiana*, the downregulation of the PLE orthologs (*AtSHP* in *Arabidopsis*, *NbSHP* in *N. benthamiana*), or the overexpression of the FUL orthologs (*AtFUL* in *Arabidopsis*, *NtFUL* in *N. sylvestris*) produce nearly identical effects in fruit dehiscence and lignification. It is very unlikely that this regulatory network directing dehiscence zone formation has been established twice during eudicot evolution, and therefore, it can be proposed that this network was already present in the common ancestor of asterids and rosids.

Recent studies of the *PLE/SHP* ortholog *TAGL1* in tomato, another Solanaceae species with fleshy fruits, have shown that *TAGL1* is required for fruit ripening (Giménez *et al.* 2010, Itkin *et al.* 2009, Pan *et al.* 2010, Vrebalov *et al.* 2009). Also, expression analyses of *FUL* and *PLE/SHP* orthologs in peach (rosid species with fleshy fruits) suggest a conserved function of these genes in controlling peach fruit lignification (Tani *et al.* 2007). A wealth of studies mapping fleshy-to-dry or dry-to-fleshy transformations into phylogenetic trees suggest that these have occurred multiple times within most main taxa of Angiosperms (cited in Pabon-Mora and Litt 2011). The likely role of the FUL-SHP network in fleshy fruit development across rosids and asterids, together with the conserved role of this same gene network directing dehiscence zone formation in distantly related species such as *Arabidopsis* and *Nicotiana* allows us to draw two main conclusions: First, it strongly supports the idea of an ancestral

subfunctionalization of PLE-like genes to direct late fruit development that would predate the divergence of rosids and asterids. Second, it points to a common evolutionary origin of dehiscence in dry fruits and ripening in fleshy fruits that would place the genetic switch that allows transformation of dry capsules into fleshy fruits and vice versa downstream of the FUL-SHP genetic network.

EXPERIMENTAL PROCEDURES

Plant material and growth condition

Nicotiana benthamiana plants were grown in the greenhouse, at 22°C (day) and 18°C (night) with a 16-h light/8-h dark photoperiod, in soil irrigated with Hoagland no. 1 solution supplemented with oligo elements (Hewitt, 1966).

Cloning and sequence analyses

Full-length coding sequence of *N. benthamiana AG* and *PLE* genes have been isolated by RT-PCR on cDNA of young flowers of *N. benthamiana* using available sequence information of *AG-like* genes from the close relative *Nicotiana tabacum* and the more distant tomato (*Solanum lycopersicum*). From the sequence of *NAG1* (*N. tabacum AG* ortholog, accession number L23925) the oligos NbAGFor and NbAGRev were designed and used to isolate the gene *NbAG* (accession number JQ699177). From the sequence of *TAGL1* (Tomato *PLE* orthologous, accession number AY098735) and the partial sequence of *NtPLE36* (*N. tabacum PLE* ortholog, accession number U63163) the oligos NbSHPFor5'ATG and NbSHPRev were designed and used to amplify a partial sequence of *NbSHP*. The 3'end of *NbSHP* was then isolated by RT-PCR using the primers NbSHPFor2 and RT (sequence present in the oligodT primer used for retrotranscription). NbSHP has been deposited to Genbank with accession number JQ699178.

For the phylogenetic tree, the deduced amino acid sequences were aligned using the CLUSTALW tool in MACVECTOR 12.0 software (MacVector, Inc.,

http://www.macvector.com/) and further refined by hand. Pairwise Poisson genetic

distances were estimated from the alignment and a neighbour joining tree was

estimated from distance matrices from 10,000 bootstrap replicates and rooted to

OsMADS13, an *Oryza sativa* ortholog of the *Arabidopsis* class-D gene *SEEDSTICK*.

The second introns were obtained by PCR using the primers NbAGintronFor and

NbAGintronRev, in the case of *NbAG* (accession number JQ699179), NbSHPintronF

and NbSHPintronR in the case of *NbSHP* (accession number JQ699180). To predict

the probability of presence of LFY binding sites in the intron sequences we used the

Morpheus webpage facility (http://biodev.cea.fr/morpheus/Default.aspx) with the LFY

matrix. The score program permits to localize the best transcription factor binding sites

in DNA fragments. The occupancy program calculates the expected number of bound

transcription factor molecules of a DNA fragment using a biophysical model that

integrates the different binding sites present on the fragment. See table S1 for primer

sequences.

In situ hybridization

RNA *in situ* hybridization with digoxigenin-labeled probes was performed on 8-μm

paraffin sections of *N. benthamiana* buds as described by Ferrándiz et al. (2000). The

RNA antisense and sense probes were generated from a 504-bp fragment of the *NbAG*

cDNA (positions 244 to 747) and *NbSHP* from a 510-bp fragment (positions 244 to

754). Both fragments were cloned into the pGemT-Easy vector (Promega), and sense

and antisense probes were synthesized using the corresponding SP6 or T7

polymerases.

Virus-Induced Gene Silencing (VIGS) in *N. benthamiana*

The same regions of *NbAG* and *NbSHP* coding sequence used for *in situ* hybridization

were used for the VIGS experiments. In the case of the single gene constructions, a

Xba1 restriction site was added to the 5' end of the PCR fragment and a *BamH1*

restriction site was added to the 3' end. The amplicon was digested by *Xba1* and *BamH1* and cloned into a similarly digested pTRV2 vector. For the double gene construction the fragment of *NbAG* coding sequence was introduced into the pTRV2-NbSHP vector using the *EcoRI* restriction site. The three resulting plasmids, pTRV2-NbAG, pTRV2-NbSHP and pTRV2-NbAG-NbSHP were confirmed by digestion and sequencing, before being introduced into *Agrobacterium tumefaciens* strain GV3101. The Agro inoculation of *N. bentahamiana* leaves was performed as described (Dinesh-Kumar *et al.* 2003).

Quantitative RT-PCR

Total RNA was extracted from flowers at anthesis with the RNeasy Plant Mini kit (Qiagen). Four micrograms of total RNA were used for cDNA synthesis performed with the First-Strand cDNA Synthesis kit (Invitrogen) and the qPCR master mix was prepared using the iQTM SYBR Green Supermix (Bio-rad). The primers used to amplify *NbAG* (qNbAGFor and qNbAGRev) and *NbSHP* (qNbSHPFor and qNbSHPRev) generated products of 81 bp and did not show any cross-amplification. Results were normalized to the expression of the *Elongation Factor 1* (*EF1*) mRNA (accession number AY206004), amplified by qNbEF1for and qNbEF1rev. The efficiency in the amplification of *NbAG*, *NbSHP* and the *EF1* reference gene was similar. The PCR reactions were run and analyzed using the ABI PRISM 7700 Sequence detection system (Applied Biosystems). See Table S1 for primers sequences.

Scanning electron microscopy (SEM) and histology

VIGS-treated plants were analyzed by CryoSEM on fresh tissue under the microscope JEOL, model JSM 5410, CRIOSEM Instrument CT 15000-C (Oxford Instruments). Young buds were collected for histological analyses, fixed in FAA under vacuum and embedded into paraffin. 10-μm ections were stained in a 0.2% toluidine blue solution

and observed under a microscope Nikon Eclipse E-600. For lignin observation, fruits were fixed in FAA, stained for 5 min in 2.5% phloroglucinol and soaked 30 sec in 50% HCl.

SUPPORTING INFORMATION

Figure S1. Analyses of *NbAG* and *NbSHP* second intron.

Figure S2.Sense controls for i*n situ* hybridization .

Figure S3. Expression level of *NbAG* and *NbSHP* by real time PCR analysis in TRV2-NbAG, TRV2-NbSHP or TRV2-NbAG-NbSHP flowers

Figure S4. Additional phenotypes of NbSHP-VIGS flowers.

Figure S5. Morphology of indehiscent NbSHP-VIGS fruits

Table S1. Primers used in this work

REFERENCES

Airoldi, C.A., Bergonzi, S. and Davies, B. (2010) Single amino acid change alters the ability to specify male or female organ identity. *Proc Natl Acad Sci USA*, **107**, 18898-18902.

Bowman, J.L., Smyth, D.R. and Meyerowitz, E.M. (1989) Genes directing flower development in Arabidopsis. *Plant Cell*, **1**, 37-52.

Bradley, D., Carpenter, R., Sommer, H., Hartley, N. and Coen, E. (1993) Complementary floral homeotic phenotypes result from opposite orientations of a transposon at the plena locus of Antirrhinum. *Cell*, **72**, 85-95.

Busch, M.A., Bomblies, K. and Weigel, D. (1999) Activation of a floral homeotic gene in Arabidopsis. *Science*, **285**, 585-587.

Causier, B., Bradley, D., Cook, H. and Davies, B. (2009) Conserved intragenic elements were critical for the evolution of the floral C-function. *Plant J*, **58**:41-52.

Causier, B., Castillo, R., Zhou, J., Ingram, R., Xue, Y., Schwarz-Sommer, Z. and Davies, B. (2005) Evolution in action: following function in duplicated floral homeotic genes. *Curr Biol*, **15**, 1508-1512.

Coen, E.S. and Meyerowitz, E.M. (1991) The war of the whorls: genetic interactions controlling flower development. *Nature*, **353**, 31-37.

Colombo, M., Brambilla, V., Marcheselli, R., Caporali, E., Kater, M. and Colombo, L. (2010) A new role for the SHATTERPROOF genes during Arabidopsis gynoecium development. *Dev Biol.***337**: 294-302.

Constantin, G.D., Krath, B.N., MacFarlane, S.A., Nicolaisen, M., Johansen, I.E. and Lund, O.S. (2004) Virus-induced gene silencing as a tool for functional genomics in a legume species. *Plant J*, **40**, 622-631.

Davies, B., Motte, P., Keck, E., Saedler, H., Sommer, H. and Schwarz-Sommer, Z. (1999) PLENA and FARINELLI: redundancy and regulatory interactions between two Antirrhinum MADS-box factors controlling flower development. *EMBO J*, **18**, 4023-4034.

Dreni, L., Pilatone, A., Yun, D., Erreni, S., Pajoro, A., Caporali, E., Zhang, D. and Kater, M.M. (2011) Functional Analysis of All AGAMOUS Subfamily Members in Rice Reveals Their Roles in Reproductive Organ Identity Determination and Meristem Determinacy. *Plant Cell*, **23**: 2850-63

Dinesh-Kumar, S.P., Anandalakshmi, R., Marathe, R., Schiff, M. and Liu Y. (2003) Virus-Induced Gene Silencing. PLANT FUNCTIONAL GENOMICS Methods in Molecular Biology, Volume 236, III, 287-293.

Ferrándiz, C. (2002) Regulation of fruit dehiscence in Arabidopsis. *Journal of Experimental Botany*, **53:** 2031-2038.

Ferrandiz, C., Fourquin, C., Prunet, N., Scutt, C., Sundberg, E., Trehin, C. and Vialette-Guiraud, A. (2010) Carpel Development. *Advances in Botanical Research*, **55**, 1-74.

Ferrándiz, C., Liljegren, S.J. and Yanofsky, M.F. (2000) Negative regulation of the SHATTERPROOF genes by FRUITFULL during Arabidopsis fruit development. *Science*, **289**, 436-438.

Giménez, E., Pineda, B., Capel, J., Antón, M.T., Atarés, A., Pérez-Martín, F., García-Sogo, B., Angosto, T., Moreno, V. and Lozano, R. (2010) Functional analysis of the Arlequin mutant corroborates the essential role of the Arlequin/TAGL1 gene during reproductive development of tomato. *PLoS ONE*, **5**, e14427.

Hewitt, Y. (1966) Sand and water culture methods used in the study of plant nutrition, Farnham, UK: Commonwealth Agricultural Bureau.

Hileman, L.C., Drea, S., Martino, G., Litt, A. and Irish, V.F. (2005) Virus-induced gene silencing is an effective tool for assaying gene function in the basal eudicot species Papaver somniferum (opium poppy). *Plant J*, **44**, 334-341.

Hong, R.L., Hamaguchi, L., Busch, M.A. and Weigel, D. (2003) Regulatory elements of the floral homeotic gene AGAMOUS identified by phylogenetic footprinting and shadowing. *Plant Cell*, **15**, 1296–1309.

Itkin, M., Seybold, H., Breitel, D., Rogachev, I., Meir, S. and Aharoni, A. (2009) The TOMATO AGAMOUS-LIKE 1 is a Component of the Fruit Ripening Regulatory Network. *Plant J*, **60**:1081-95.

Kapoor, M., Tsuda, S., Tanaka, Y., Mayama, T., Okuyama, Y., Tsuchimoto, S. and Takatsuji, H. (2002) Role of petunia pMADS3 in determination of floral organ and meristem identity, as revealed by its loss of function. *Plant J*, **32**, 115-127.

Kater, M.M., Colombo, L., Franken, J., Busscher, M., Masiero, S., Van Lookeren Campagne, M.M., Angenent, G.C. (1998) Multiple AGAMOUS homologs from cucumber and petunia differ in their ability to induce reproductive organ fate. *Plant Cell*, **10**, 171-182.

Kempin, S.A., Mandel, M.A. and Yanofsky, M.F. (1993) Conversion of perianth into reproductive organs by ectopic expression of the tobacco floral homeotic gene NAG1. *Plant Physiol*, **103**, 1041-1046.

Kramer, E.M., Jaramillo, M.A. and Di Stilio, V.S. (2004) Patterns of gene duplication and functional evolution during the diversification of the AGAMOUS subfamily of MADS box genes in angiosperms. *Genetics*, **166**, 1011-1023.

Liljegren, S.J., Ditta, G.S., Eshed, Y., Savidge, B., Bowman, J.L. and Yanofsky, M.F. (2000) SHATTERPROOF MADS-box genes control seed dispersal in Arabidopsis. *Nature*, **404**, 766-770.

Mandel, M.A., Bowman, J.L., Kempin, S.A., Ma, H., Meyerowitz, E.M. and Yanofsky, M.F. (1992) Manipulation of flower structure in transgenic tobacco. *Cell*, **71**, 133-143.

Mena, M., Ambrose, B.A., Meeley, R.B., Briggs, S.P., Yanofsky, M.F. and Schmidt, R.J. (1996) Diversification of C-function activity in maize flower development. *Science*, **274**, 1537-1540.

Mizukami, Y. and Ma, H. (1992) Ectopic expression of the floral homeotic gene AGAMOUS in transgenic Arabidopsis plants alters floral organ identity. *Cell*, **71**, 119-131.

Moyroud, E., Minguet, E.G., Ott, F., Yant, L., Posé, D., Monniaux, M., Blanchet, S., Bastien, O., Thévenon, E., Weigel, D., Schmid, M. and Parcy, F. (2011) Prediction

of Regulatory Interactions from Genome Sequences Using a Biophysical Model for the Arabidopsis LEAFY Transcription Factor. *Plant Cell*. **23**:1293-306.

Pabon-Mora, N. and Litt, A. (2011) Comparative anatomical and developmental analysis of dry and fleshy fruits of Solanaceae. *American Journal of Botany*, **98**, 1415-1436.

Pan, I.L., McQuinn, R., Giovannoni, J.J. and Irish, V.F. (2010) Functional diversification of AGAMOUS lineage genes in regulating tomato flower and fruit development. *J Exp Bot.*, **61**:1795-806.

Parcy, F., Nilsson, O., Busch, M.A., Lee, I. and Weigel, D. (1998) A genetic framework for floral patterning. *Nature*, **395**, 561-566.

Pnueli, L., Hareven, D., Rounsley, S.D., Yanofsky, M.F. and Lifschitz, E. (1994) Isolation of the tomato AGAMOUS gene TAG1 and analysis of its homeotic role in transgenic plants. *Plant Cell*, **6**, 163-173.

Ratcliff, F., Martin-Hernandez, A.M. and Baulcombe, D.C. (2001) Technical Advance. Tobacco rattle virus as a vector for analysis of gene function by silencing. *Plant J*, **25**, 237-245.

Smykal, P., Gennen, J., De Bodt, S., Ranganath, V. and Melzer, S. (2007) Flowering of strict photoperiodic Nicotiana varieties in non-inductive conditions by transgenic approaches. *Plant Mol Biol*, **65**, 233-242.

Tani, E., Polidoros, A.N. and Tsaftaris, A.S. (2007) Characterization and expression analysis of FRUITFULL- and SHATTERPROOF-like genes from peach (Prunus persica) and their role in split-pit formation. *Tree Physiol*, **27**, 649-659.

Vrebalov, J., Pan, I.L., Arroyo, A.J.M., McQuinn, R., Chung, M., Poole, M., Rose, J., Seymour, G., Grandillo, S., Giovannoni, J. and Irish, V.F. (2009) Fleshy fruit expansion and ripening are regulated by the Tomato SHATTERPROOF gene TAGL1. *Plant Cell*, **21**, 3041-3062.

Wege, S., Scholz, A., Gleissberg, S. and Becker, A. (2007) Highly efficient virus-induced gene silencing (VIGS) in California poppy (Eschscholzia californica): an evaluation of VIGS as a strategy to obtain functional data from non-model plants. *Annals of Botany*, **100**, 641-649.

Yellina, A.L., Orashakova, S., Lange, S., Erdmann, R., Leebens-Mack, J. and Becker, A. (2010) Floral homeotic C function genes repress specific B function genes in the carpel whorl of the basal eudicot California poppy (Eschscholzia californica). *Evodevo*, **1**, 13.

Zahn, L.M., Leebens-Mack, J.H., Arrington, J.M., Hu, Y., Landherr, L.L., dePamphilis, C.W., Becker, A., Theissen, G. and Ma, H. (2006) Conservation and divergence in the AGAMOUS subfamily of MADS-box genes: evidence of independent sub- and neofunctionalization events. *Evol Dev.,* **8**, 30-45.

FIGURE LEGENDS

Figure 1

(a) Phylogenetic tree from the protein sequences of AG and PLE homologues, AG (X53579), EScaAG1 (DQ088996), EScaAG2 (DQ088997), AmFAR (AJ239057), FBP6 (X68675), OsMADS3 (L37528), OsMADS13 (AF151693), OsMADS58 (AB232157), PLE (S53900), pMADS3 (X72912), PPERSHP (DQ777635), AtSHP1 (M55550), AtSHP2 (M55553), TAG1 (L26295), TAGL1 (AY098735) Numbers on branches indicate bootstrap values for 10000 replicates. The gene *OsMADS13*, *Oryza sativa* ortholog of the *Arabidopsis* class-D gene *SEEDSTICK*, was used as outgroup in this analysis. Sequences belonging to euAG and euPLE lineages are shadowed in light grey and dark grey respectively. (b) Prediction of LFY occupancy of the largest intron of *AG* and *PLE* homologues from *Arabidopsis* (*AtAG* At4g18960, *AtSHP1* At3g58780 and *AtSHP2* At2g42830), *Antirrhinum* (*AmPLE* AY935269 and *AmFAR* AJ239057) and *N.*

benthamiana (*NbAG* and *NbSHP*). The occupancy calculates the relative expected number of bound LFY molecules of each DNA sequence integrating the different binding sites present on the fragment.

Figure 2

In situ expression analyses of *NbAG* and *NbSHP* in wild type *N. benthamiana* floral buds. Sections on the left were probed with *NbAG* (a, c, e, g and i). All sections on the right were probed with *NbSHP* (b, d, f, h and j).

(a-b) *NbAG* and *NbSHP* expression restricted in the center of the floral meristem at stage 2 when sepal primordia are clearly visible. (c-d) Expression remains in the center of the floral meristem in stage 4 flowers, when petals begin to form. (e-f) In stage 6 flowers, expression is specific to the developing sexual organs. (g-h) In mature flowers, expression is detected in ovules, placenta, carpel wall and weakly in stamens. (i-j) In later stages, expression is mainly detected in ovules. s: sepal, p: petal, st: stamen, pi: pistil, o: ovule. Developmental stages from Mandel et al. (1992). Control hybridizations with sense probes are shown in Figure S2.

Figure 3

Phenotypes of *N. benthamiana* plants treated with pTRV2-NbAG, pTRV2-NbSHP or pTRV2-NbAG-NbSHP.

(a) to (d) Top view of *N. benthamiana* flowers. (a) Wild type flower in anthesis presenting five petals and five anthers surrounding the stigma. (b) NbAG-VIGS flower showing the conversion of stamens into petals and no visible stigma. (c) NbSHP-VIGS flower. Note the absence of stigma in the center of the five anthers. (d) NbAG-NbSHP-VIGS flower presenting additional whorls of petals and no visible sexual organs. (e) to (i) Longitudinal section of *N. benthamiana* flowers. (e) Wild type anthesis flower presenting consecutively a whorl of sepals, a tubular whorl of petals, then the stamens

whose filaments are adnately fused to the petals, and the central pistil. (f) NbAG-VIGS flower showing homeotic conversions of stamens into petals and the presence of an abnormal fourth whorl. (g) NbSHP-VIGS flower presenting a pistil with an unfused and reduced style. (h) and (i) NbAG-NbSHP-VIGS flowers. In both flowers stamens are replaced by petals. (h) The fourth whorl is composed of petals. (i) In the center of the flower develops a new whorl of sepals enclosing petals. (j) to (o) Floral organs at the fourth whorl of *N. benthamiana* flowers. (j) Wild type pistil composed of an "egg-shaped" ovary, a long style and a flat stigma. (k) to (m) Central whorl of a NbAG-VIGS flower. (k) Absence of ovary and style differentiation in the highly modified fourth whorl of the NbAG-VIGS flower. (l) Opened fourth whorl of a NbAG-VIGS flower revealing the presence of inner petals. (m) Closer view of the apical part of the fourth whorl of a NbAG-VIGS flower indicating the presence of stigmatic tissue. (n) NbSHP-VIGS *N. benthamiana* pistils showing fusion defects, reduction of style length and increased number of styles and stigma. (o) Presence of an ectopic floral meristem at the base of the fourth whorl in a NbAG-NbSHP-VIGS flower. Scale bar = 0.5 cm.

Figure 4

Sections of *N. benthamiana* flowers from plants treated with pTRV2-NbAG, pTRV2-NbSHP or pTRV2-NbAG-NbSHP.

(a) to (d) Transverse section of *N. benthamiana* flower at 0.5 cm up from the pedicel. (a) wild type flower showing an external sepal whorl, a tubular petal whorl with five adnately fused stamens filaments and the bi-carpellate central ovary. (b) Transverse section of a NbSHP-VIGS flower presenting wild type first and second whorls, eight stamen filaments fused with the petals and at least five carpels developing in the ovary. (c) Transverse section of a NbAG-VIGS flower showing a normal first whorl of sepals, an enlarged second whorl of petals surrounding eight stamens converted into free petals and a fourth whorl lacking carpel tissue differentiation, ovules and placenta. (d)

Transverse section of a NbAG-NbSHP-VIGS flower lacking sexual organs and composed of an outer whorl of sepals and numerous whorls of petals. (e) and (f) Longitudinal section of the apical part of the pistil. (e) WT stigma and upper style. (f) NbSHP-VIGS with unfused style and stigma. (g) Longitudinal section of a wild type *N. benthamiana* flower. (h) and (i) Longitudinal section of NbAG-VIGS flower. (h) Conversion of stamens into petals and the presence of some stigmatic tissue in the fourth whorl are shown. (i) Longitudinal section of NbAG-VIGS flower showing the presence of a new floral meristem in the center of the flower. (j) Longitudinal section of a NbSHP-VIGS gynoecium presenting additional whorls of carpels developing in its center, and numerous styles. cw: carpel wall, fm: floral meristem, ov: ovary, p: petal, p*: free petal, s: sepal, sg: stigma, sy: style.

Figure 5

Scanning electron microscope analyses of epidermal cell morphology in flowers of VIGS *N.benthamiana* treated plants. (a) Small and rectangular cells of a wild type ovary. (b) Elongated cells of a wild type style. (c) Puzzle shaped cells, trichomes and stomata of a wild-type sepal. (d) Cellular types at the surface of VIGS NbAG fourth whorl. Cells are irregular and trichomes and stomata can be observed. (e) and (f) Cellular types observed in a VIGS NbSHP fourth whorl, in the ovary (e) and in the style (f). Note the presence of trichomes and stomata in both cases. Scale bar = 60μm.

Figure 6

Fruit dehiscence and lignification altered in *N. benthamiana* plants treated with pTRV2-NbSHP. (a) Open mature capsule of a *N. benthamiana* wild-type plant. (b) Closed mature capsule of a NbSHP-VIGS plant. (c) Lignification pattern of a *N. benthaniana* wild-type fruit. (d) Absence of lignin of a *N. benthamiana* NbSHP-VIGS fruit.
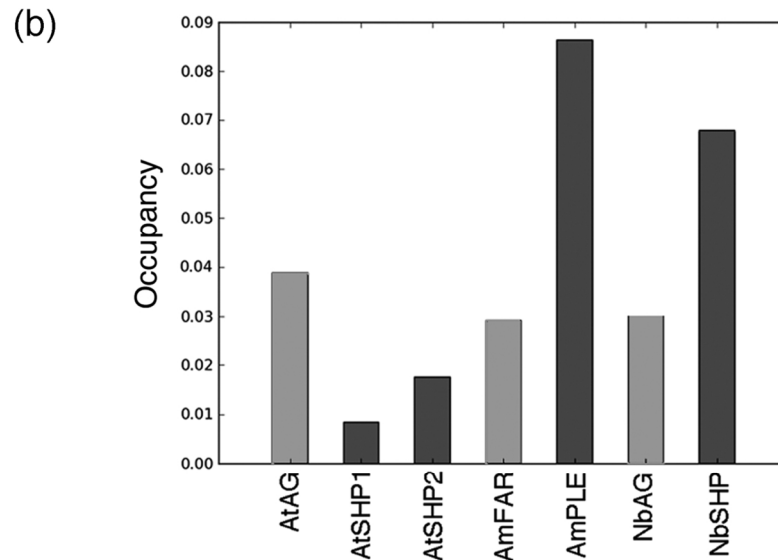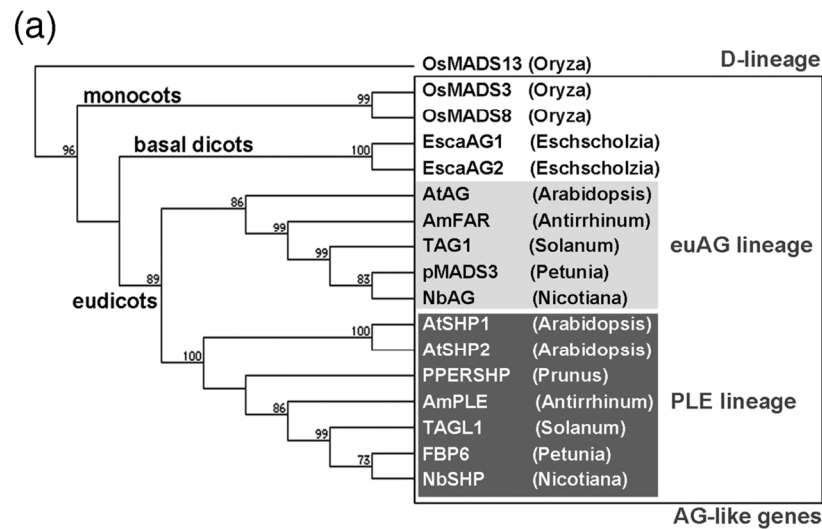
Figure 1. (a) Phylogenetic tree from the protein sequences of AG and PLE homologues, AG (X53579), EScaAG1 (DQ088996), EScaAG2 (DQ088997), AmFAR (AJ239057), FBP6 (X68675), OsMADS3 (L37528), OsMADS13 (AF151693), OsMADS58 (AB232157), PLE (S53900), pMADS3 (X72912), PPERSHP (DQ777635), AtSHP1 (M55550), AtSHP2 (M55553), TAG1 (L26295), TAGL1 (AY098735) Numbers on branches indicate bootstrap values for 10000 replicates. The gene OsMADS13, Oryza sativa ortholog of the Arabidopsis class-D gene SEEDSTICK, was used as outgroup in this analysis. Sequences belonging to euAG and euPLE lineages are shadowed in light grey and dark grey respectively. (b) Prediction of LFY occupancy of the largest intron of AG and PLE homologues from Arabidopsis (AtAG At4g18960, AtSHP1 At3g58780 and AtSHP2 At2g42830), Antirrhinum (AmPLE AY935269 and AmFAR AJ239057) and N. benthamiana (NbAG and NbSHP). The occupancy calculates the relative expected number of bound LFY molecules of each DNA sequence integrating the different binding sites present on the fragment.
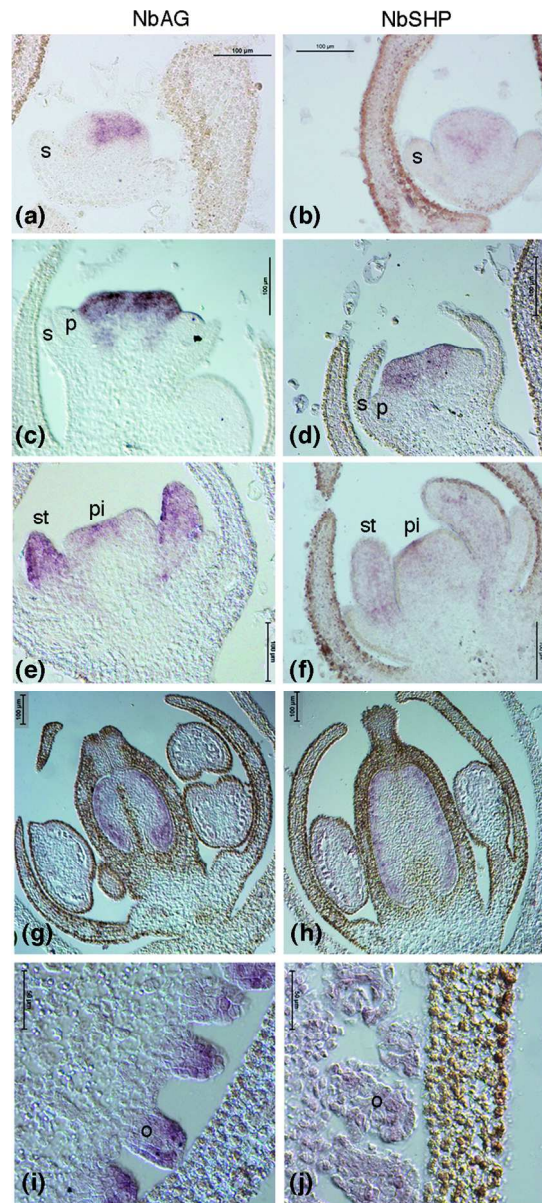
115x165mm (300 x 300 DPI)

Figure 2. In situ expression analyses of NbAG and NbSHP in wild type N. benthamiana floral buds. Sections on the left were probed with NbAG (a, c, e, g and i). All sections on the right were probed with NbSHP (b, d, f, h and j).
(a-b) NbAG and NbSHP expression restricted in the center of the floral meristem at stage 2 when sepal primordia are clearly visible. (c-d) Expression remains in the center of the floral meristem in stage 4 flowers, when petals begin to form. (e-f) In stage 6 flowers, expression is specific to the developing sexual organs. (g-h) In mature flowers, expression is detected in ovules, placenta, carpel wall and weakly in stamens. (i-j) In later stages, expression is mainly detected in ovules. s: sepal, p: petal, st: stamen, pi: pistil, o: ovule. Developmental stages from Mandel et al. (1992). Control hybridizations with sense probes are shown in Figure S2.
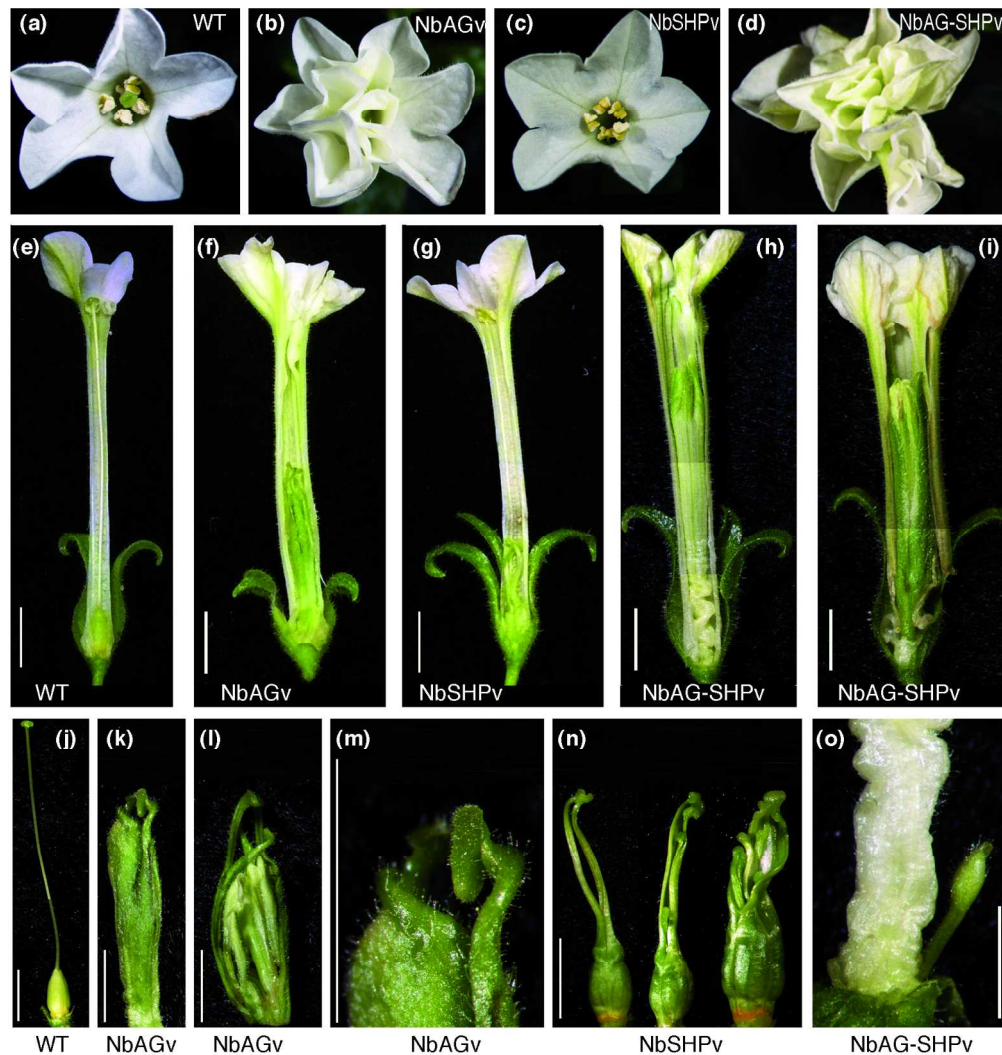77x173mm (300 x 300 DPI)

Figure 3. Phenotypes of N. benthamiana plants treated with pTRV2-NbAG, pTRV2-NbSHP or pTRV2-NbAG-NbSHP.
(a) to (d) Top view of N. benthamiana flowers. (a) Wild type flower in anthesis presenting five petals and five anthers surrounding the stigma. (b) NbAG-VIGS flower showing the conversion of stamens into petals and no visible stigma. (c) NbSHP-VIGS flower. Note the absence of stigma in the center of the five anthers. (d) NbAG-NbSHP-VIGS flower presenting additional whorls of petals and no visible sexual organs. (e) to (i) Longitudinal section of N. benthamiana flowers. (e) Wild type anthesis flower presenting consecutively a whorl of sepals, a tubular whorl of petals, then the stamens whose filaments are adnately fused to the petals, and the central pistil. (f) NbAG-VIGS flower showing homeotic conversions of stamens into petals and the presence of an abnormal fourth whorl. (g) NbSHP-VIGS flower presenting a pistil with an unfused and reduced style. (h) and (i) NbAG-NbSHP-VIGS flowers. In both flowers stamens are replaced by petals. (h) The fourth whorl is composed of petals. (i) In the center of the flower develops a new whorl of sepals enclosing petals. (j) to (o) Floral organs at the fourth whorl of N. benthamiana flowers. (j) Wild type pistil composed of an "egg-shaped" ovary, a long style and a flat stigma. (k) to (m) Central whorl of a NbAG-VIGS flower. (k) Absence of ovary and style differentiation in the highly modified fourth whorl of the NbAG-VIGS flower. (l) Opened fourth whorl of a NbAG-VIGS flower revealing the presence of inner petals. (m) Closer view of the apical part of the fourth whorl of a NbAG-VIGS flower indicating the presence of stigmatic tissue. (n) NbSHP-VIGS N. benthamiana pistils showing fusion defects, reduction of style length and increased

number of styles and stigma. (o) Presence of an ectopic floral meristem at the base of the fourth whorl in a
NbAG-NbSHP-VIGS flower. Scale bar = 0.5 cm.
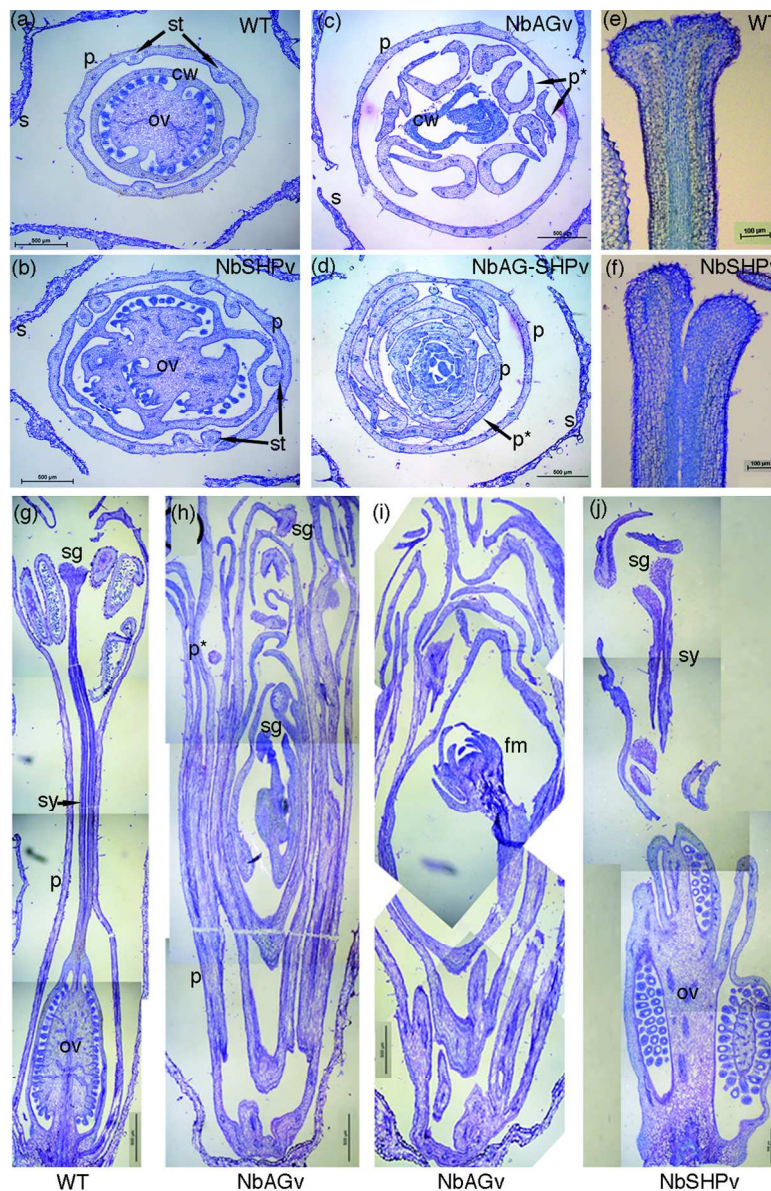161x172mm (300 x 300 DPI)

Figure 4. Sections of N. benthamiana flowers from plants treated with pTRV2-NbAG, pTRV2-NbSHP or pTRV2-NbAG-NbSHP.
(a) to (d) Transverse section of N. benthamiana flower at 0.5 cm up from the pedicel. (a) wild type flower showing an external sepal whorl, a tubular petal whorl with five adnately fused stamens filaments and the bi-carpellate central ovary. (b) Transverse section of a NbSHP-VIGS flower presenting wild type first and second whorls, eight stamen filaments fused with the petals and at least five carpels developing in the ovary. (c) Transverse section of a NbAG-VIGS flower showing a normal first whorl of sepals, an enlarged second whorl of petals surrounding eight stamens converted into free petals and a fourth whorl lacking carpel tissue differentiation, ovules and placenta. (d) Transverse section of a NbAG-NbSHP-VIGS flower lacking sexual organs and composed of an outer whorl of sepals and numerous whorls of petals. (e) and (f) Longitudinal section of the apical part of the pistil. (e) WT stigma and upper style. (f) NbSHP-VIGS with unfused style and stigma. (g) Longitudinal section of a wild type N. benthamiana flower. (h) and (i) Longitudinal section of NbAG-VIGS flower. (h) Conversion of stamens into petals and the presence of some

stigmatic tissue in the fourth whorl are shown. (i) Longitudinal section of NbAG-VIGS flower showing the presence of a new floral meristem in the center of the flower. (j) Longitudinal section of a NbSHP-VIGS gynoecium presenting additional whorls of carpels developing in its center, and numerous styles. cw: carpel wall, fm: floral meristem, ov: ovary, p: petal, p*: free petal, s: sepal, sg: stigma, sy: style.
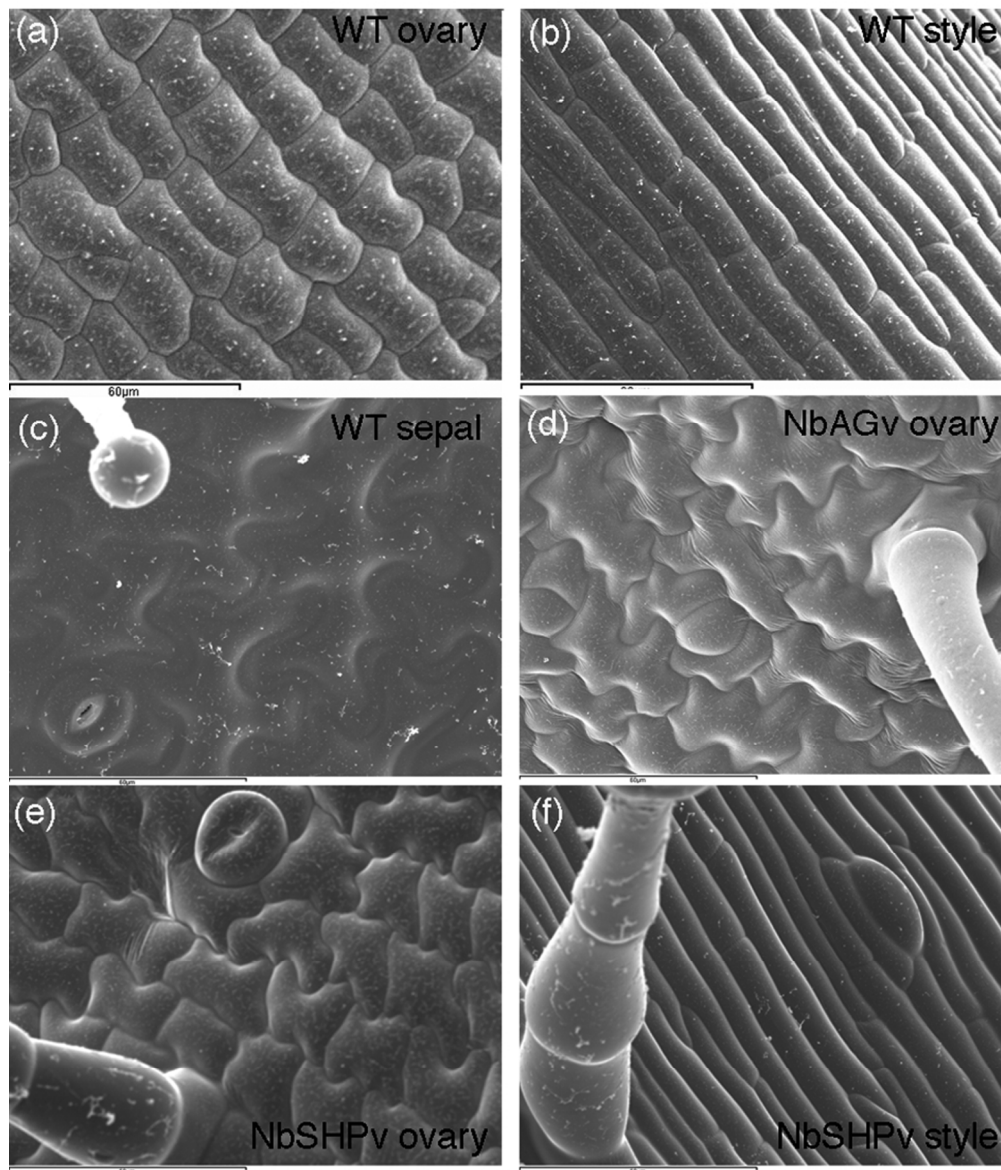102x160mm (300 x 300 DPI)

Figure 5. Scanning electron microscope analyses of epidermal cell morphology in flowers of VIGS N.benthamiana treated plants. (a) Small and rectangular cells of a wild type ovary. (b) Elongated cells of a wild type style. (c) Puzzle shaped cells, trichomes and stomata of a wild-type sepal. (d) Cellular types at the surface of VIGS NbAG fourth whorl. Cells are irregular and trichomes and stomata can be observed. (e) and (f) Cellular types observed in a VIGS NbSHP fourth whorl, in the ovary (e) and in the style (f). Note the presence of trichomes and stomata in both cases. Scale bar = 60µm.
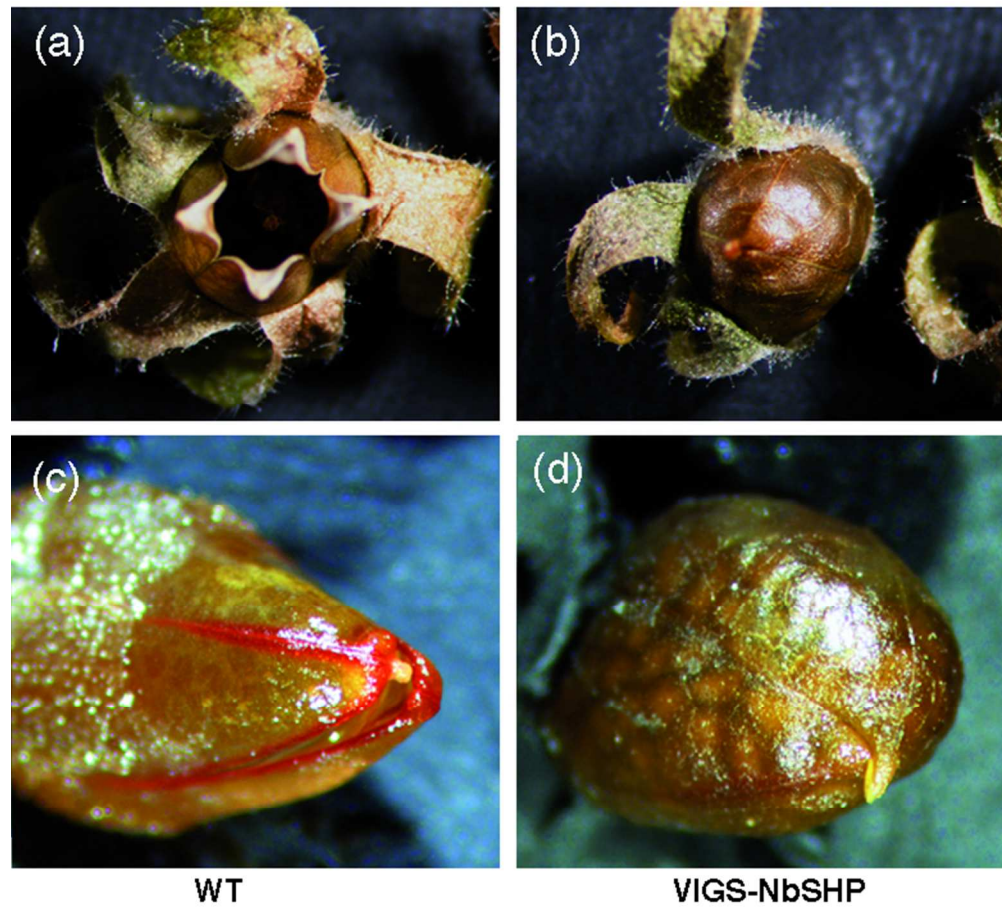
80x94mm (300 x 300 DPI)

Figure 6. Fruit dehiscence and lignification altered in N. benthamiana plants treated with pTRV2-NbSHP. (a) Open mature capsule of a N. benthamiana wild-type plant. (b) Closed mature capsule of a NbSHP-VIGS plant. (c) Lignification pattern of a N. benthaniana wild-type fruit. (d) Absence of lignin of a N. benthamiana NbSHP-VIGS fruit.

66x60mm (300 x 300 DPI)

Supplementary material

<u>Figure S1</u>

Analyses of *NbAG* and *NbSHP* second intron. (a) Schematic representation of *NbAG* and *NbSHP* second intron. The squares represent the conserved motifs : the aAGAAT box (A) and the CCAATCA repeat motifs (B), the grey circle symbolizes the putative LFY-binding site. (b) and (c) Alignment of the intronic conserved region of the second intron of *AtAG* (At4g18960), *AmPLE* (AY935269), *AmFAR* (AJ239057), *NbAG* (JQ699177) and *NbSHP* (JQ699178). (b) The aAGAAT box (A). (c) The conserved LFY binding site (underlined in grey) and the CCAATCA repeat motifs (B, underlined in black). (e) and (f) Scores and localization of the predicted LFY binding sites in *NbAG* second intron (e) and in *NbSHP* second intron (f). The position of the conserved motifs described in (a-c) are indicated by arrows.

<u>Figure S2</u>. Sense controls for i*n situ* hybridization

In situ hybridization performed on longitudinal sections of wild type *N. benthamiana* floral buds with sense probes. (a) stage 4. (b) stage 6. (c) mature flower. (d) close up of the ovule of a mature flower.

<u>Figure S3</u>

Expression level of *NbAG* and *NbSHP* by real time PCR analyses in flowers of WT and 5 different plants inoculated by TRV2-NbAG (NbAGv), TRV2-NbSHP (NbSHPv) or TRV2-NbAG-NbSHP (NbAG-NbSHPv).

<u>Figure S4</u>. Additional phenotypes of NbSHP-VIGS and NbAG-SHPv flowers.

Top view of *N. benthamiana* flowers. (a) Wild type flower. (b) NbSHP-VIGS flower showing a mild conversion of stamens into petals (arrow). (c) NbAG-SHP-VIGS flower with 6 petals in the second whorl. (d) Transversal section of a NbAG-SHP-VIGS flower with 6 sepals in the first whorl

Figure S5

Morphology of indehiscent NbSHP-VIGS fruits. (a) to (e) Transversal sections. (a) WT ovary at anthesis. (b) NbSHP-VIGS ovary at anthesis. (c) WT sepal at anthesis. (d) WT mature fruit wall. (e) NbSHP-VIGS mature fruit wall. (f) to (k) Scanning electron microscope photographs. (f) and (i) Dehiscence zone of the WT mature fruit. (g) and (j) Apical part of the indehiscent NbSHP-VIGS mature fruit . (h) and (k) WT sepal.